HHS Public Access

Author manuscript

JAMA Ophthalmol. Author manuscript; available in PMC 2016 August 09.

Published in final edited form as:

JAMA Ophthalmol. 2016 June 1; 134(6): 697–702. doi:10.1001/jamaophthalmol.2016.0874.

Optical Coherence Tomography Angiography in Choroideremia:

Correlating Choriocapillaris Loss With Overlying Degeneration

Nieraj Jain, MD, **Yali Jia, PhD**, **Simon S. Gao, PhD**, **Xinbo Zhang, PhD**, **Richard G. Weleber, MD**, **David Huang, MD, PhD**, and **Mark E. Pennesi, MD**

Department of Ophthalmology, Emory University, Atlanta, Georgia (Jain); Casey Eye Institute, Oregon Health & Science University, Portland (Jain, Jia, Gao, Weleber, Huang, Pennesi); Division of Biostatistics, Department of Public Health and Preventive Medicine, Oregon Health & Science University, Portland (Zhang)

Abstract

Importance—Novel therapies for choroideremia, an X-linked recessive chorioretinal degeneration, demand a better understanding of the primary site(s) of cellular degeneration. Optical coherence tomography angiography allows for choriocapillaris (CC) imaging. We compared the extent of structural alterations of the CC, retinal pigment epithelium, and photoreceptors with multimodal imaging.

Corresponding Author: Mark E. Pennesi, MD, Casey Eye Institute, Oregon Health & Science University, 3375 SW Terwilliger Blvd. Portland, OR 97239 (pennesim@ohsu.edu).

Author Contributions: Dr Jain had full access to all of the data in the study and takes responsibility for the integrity of the data and the accuracy of the data analysis.
Study concept and design: Jain, Huang, Pennesi.
Acquisition, analysis, or interpretation of data: Jain. Jia, Gao, Zhang. Weleber, Huang.
Drafting of the manuscript: Jain, Pennesi.
Critical revision of the manuscript for important intellectual content: All authors.
Statistical analysis: Jain, Zhang.
Obtained funding: Jain. Jia, Weleber, Huang. Pennesi.
Administrative, technical, or material support: Gao.
Study supervision: Jia, Weleber, Pennesi.

Conflict of Interest Disclosures: All authors have completed and submitted the ICMJE Form for Disclosure of Potential Conflicts of Interest. Dr Jia reported receiving research equipment, research grant, and patent royalty from Optovue Inc and being a licensee on pending patent "Split-Spectrum Amplitude-Decorrelation Angiography With Optical Coherence Tomography." Dr Weleber reported receiving personal fees for consultation from Novartis and Pfizer; receiving financial support for research to Oregon Health & Science University from Sanofi; receiving research support, serving on a scientific advisory board, and receiving reimbursement for travel expenses from AGTC; receiving a grant and serving on scientific advisory boards for Foundation Fighting Blindness (this relationship has been reviewed and managed by Oregon Health & Science University); and having been issued US patent 8,657,446 for "Method and Apparatus for Visual Field Monitoring, Also Known as Visual Field Monitoring and Analysis, or VFMA." Dr Huang reported having stock options in Optovue, Inc; receiving research equipment, research grant, and patent royalty from Optovue, Inc; receiving patent royalty from Carl Zeiss Meditec, Inc; and being a licensee on pending patent "Split-Spectrum Amplitude-Decorrelation Angiography." Dr Pennesi reported serving as a consultant to AGTC, ISIS Pharmaceuticals, Sparks, and Sucampo Pharmaceuticals; receiving grant support as part of clinical trials for AGTC and Sanofi; and receiving grants from Foundation Fighting Blindness and Research to Prevent Blindness. No other disclosures were reported.

Supplemental content at jamaophthalmology.com

Previous Presentation: This paper was presented in part at the 38th Annual Meeting of the Macula Society; February 26,2015; Scottsdale, Arizona; and at the 2015 Annual Meeting of the Association for Research in Vision and Ophthalmology; May 5, 2015; Denver, Colorado.

Additional Contributions: Catie Schlechter, MS, CGC, Casey Eye Institute, Oregon Health & Science University, Portland, provided guidance with molecular testing and interpretation; she received no compensation.

Observations—In a clinical case series conducted from September 15,2014, through February 5,2015,14 eyes of 7 male patients with choroideremia (median age, 34 years [interquartile range, 15-46 years]; age range, 13-48 years), 4 eyes of 2 women with choroideremia carrier state (both in mid-50s), and 6 eyes of 6 controls (median age, 42.5 years [interquartile range, 33-55 years]; age range, 24-55 years) underwent multimodal imaging with optical coherence tomography angiography and electroretinography. The mean (SD) macular CC density was 82.9% (13.4%) in patients with choroideremia, 93.0% (3.8%) in female carriers, and 98.2% (1.3%) in controls. The mean (SD) CC density in affected eyes was higher in regions with preserved (92.6% [5.8%]) vs absent (75.9% [12.6%]) ellipsoid zone (mean difference. 16.7%; 95% CI, 12.1% to 21.3%; $P < .001$). Seventeen of 18 eyes of the patients and carriers had outer retinal tubulations forming pseudopod-like extensions from islands of preserved ellipsoid zone. Outer retinal tubulations were associated with absence of underlying retinal pigment epithelium and were longer ($r = -0.62$; 95% CI, −0.84 to −0.19; $P < .001$) and more numerous ($r = -0.71$; 95% CI, −0.91 to −0.27; $P < .001$) in more severely affected eyes.

Conclusions and Relevance—These findings suggest that regional changes in CC density correlate with photoreceptor structural alterations in choroideremia. Although closely coupled, the results suggest that retinal pigment epithelium loss is more extensive than photoreceptor loss.

Prior studies have variably implicated the retinal pigment epithelium (RPE), photoreceptors, and choriocapillaris (CC) as the primary site(s) of degeneration in choroideremia, an X-linked recessive chorioretinal degeneration.[1-5] A recent gene therapy study targeted the RPE and photoreceptors.[6] However, little is known of the role of the CC in disease progression, partly because of the difficulty with visualizing this tissue layer in vivo.

Optical coherence tomography (OCT) angiography (OCTA) permits CC imaging that is not possible with conventional angiography. We hypothesize that if coupled with en face imaging of the photoreceptors and RPE, OCTA will provide insights into the underlying pathobiology of choroideremia.

Methods

This study was conducted from September 15, 2014, through February 5, 2015, at the Oregon Health & Science University. The protocol and informed consent were approved by the Oregon Health & Science University Institutional Review Board. Written informed consent was obtained for all participants. The study adhered to the tenets of the Declaration of Helsinki[7] and complied with the Health Insurance Portability and Accountability Act.

Patients with choroideremia, choroideremia carriers, and age-matched controls underwent OCTA imaging (Avanti RTVue XR; Optovue, Inc),[8-10] fundus autofluorescence imaging (200Tx; Optos, PLC), and full-field electroretinography (ERG) (custom ERG unit).[11]

En face outer retinal OCT images were constructed from the mean reflectance from a slab spanning 45 μm to 25 μm above the Bruch membrane. En face OCTA images were constructed at varying depths, with the CC angiogram representing flow data from a 10-μm-thick slab below the Bruch membrane. To account for projection artifact from overlying

vessels, a mask of large vessels in the retinal angiogram was applied to eliminate those pixels from the CC angiogram (Figure 1).

Vessel density was computed as previously described.[12] A CC density map was constructed (Figure 1) to better quantify local CC density as follows: a grid containing 8 × 8-pixel elements was created on the angiogram, and the proportion of flow pixels within each grid element defined the CC density within that element. Linear interpolation created the final CC density map.

Following manual image registration, regions of interest were manually delineated, including the region(s) of relatively preserved RPE on fundus autofluorescence images and relatively preserved ellipsoid zone (EZ) (including pseudopodial extensions) on outer retinal OCT images (Adobe Photoshop CS6; Adobe Systems Inc). The lengths of pseudopodial extensions of EZ were measured (Figure 1B), and the longest pseudopod for each eye was selected for analysis.

Comparisons between CC density were evaluated with the Wilcoxon signed rank test; comparisons between area of preserved RPE and EZ were performed with a paired *t* test. Correlations were computed with the Pearson correlation coefficient. The generalized estimating equation approach accounted for correlation between eyes of patients (SAS version 9.4 statistical software; SAS Institute, Inc).[13]

Results

In this clinical case series, 14 eyes of 7 male patients with choroideremia (median age, 34 years [interquartile range, 15-46 years]; age range, 13-48 years), 4 eyes of 2 female carriers (both in mid-50s), and 6 eyes of 6 controls (median age, 42.5 years [interquartile range, 33-55 years]; age range, 24-55 years) were imaged. Best-corrected visual acuity ranged from 20/20 to 20/30 in affected males and 20/20 to 20/60 in female carriers (1 carrier had atrophic macular changes) (Table). The mean (SD) ERG scotopic 0.01 b-wave amplitude measured 23.0% (34.4%) (n = 12 eyes) and 121.0% (70.7%) (n = 2 eyes) of the lower limit of normal for affected and carrier eyes, respectively (eTable in the Supplement).

The mean (SD) CC density across all regions was 82.9% (13.4%) in the 14 eyes of patients with choroideremia, 93.0% (3.8%) in the 4 eyes of the carrier females, and 98.2% (1.3%) in the 6 control eyes ($P < .05$ for all between-group comparisons) (Table). The CC density was higher in regions with relatively preserved EZ as compared with regions with absence of EZ in both affected males (mean [SD], 92.6% [5.8%] vs 75.9% [12.6%], respectively; mean difference, 16.7%; 95% CI, 12.1% to 21.3%; $P < .001$; n = 14 eyes) and female carriers (mean [SD], 95.3% [0.75%] vs 81.3% [13.4%], respectively; mean difference, 14.1%; 95% CI, −7.1 to 35.2%; $P = .08$; n = 4 eyes) (Figure 2). There was a positive correlation between normalized ERG scotopic 0.01 b-wave amplitude and CC density ($r = 0.50$; 95% CI, 0.23 to 0.68; $P < .001$; n = 14 eyes).

Qualitative assessment of registered images demonstrated tight coupling of transition zones at the level of the EZ, RPE, and CC. Across all affected and carrier eyes, the mean (SD) areas of relatively preserved EZ (by OCT) and RPE (by autofluorescence) were 22.7 (9.2)

mm^2 and 20.8 (10.3) mm^2, respectively ($P < .001$; n = 15 eyes). In 14 eyes of 7 participants, the area of relatively preserved EZ was larger than the corresponding area of preserved RPE. In 2 eyes of 1 patient with choroideremia, EZ loss exceeded RPE loss by autofluorescence imaging but not by infrared reflectance imaging.

Seventeen of 18 eyes of the patients and carriers had outer retinal tubulations (ORTs). In the en face perspective, these appeared as pseudopodial extensions emanating from a central island of relatively preserved outer retina (eFigure in the Supplement). There were a mean (SD) of 13.1 (7.8) and 4.3 (5.3) ORTs within the imaged field in affected eyes and carrier eyes, respectively. There was a negative correlation between normalized ERG scotopic 0.01 b-wave amplitude and both ORT number ($r = -0.71$; 95% CI, −0.91 to −0.27; $P < .001$) and ORT length ($r = -0.62$; 95% CI, −0.84 to −0.19; $P < .001$). There was no relative preservation of CC underlying the ORTs.

Discussion

Multimodal en face imaging with OCTA demonstrated remarkably right coupling of CC loss to overlying retinal and RPE degeneration. The most severely affected eyes had distinct transition zones between relatively preserved and diseased CC, whereas carrier eyes had patchy, poorly defined regions of CC loss.

En face outer retinal imaging in these eyes revealed a unique pattern of degeneration with a central island of relatively intact photoreceptors containing pseudopodial extensions of surviving tissue. The OCT sections demonstrate that these pseudopods represent scrolled outer retina and ORTs at the margins of degeneration. In the en face perspective, the ORT is characterized by an outer hyporeflective band that originates with photoreceptor cell nuclei, adjacent to a hyperreflective line that likely originates with the external limiting membrane and inwardly migrating inner segment mitochondria.[14]

Photoreceptor layer scrolling and ORT formation suggest that the underlying RPE and/or CC is not adequately supporting the retina and that photoreceptor death is a secondary process.[14] The RPE loss exceeded the EZ loss in nearly all eyes, and ORTs consistently extended beyond the margins of preserved RPE. In more advanced cases, as measured by ERG response, ORTs were more numerous and longer. This finding suggests that with advancing degeneration, cells persist within relatively stabilized ORT structures, while the main island of retinal tissue becomes gradually smaller.

Of note, image grading was not subject to reproducibility studies, and it is unclear how these findings might vary if the same images were regraded by the same individual or others.

The split-spectrum amplitude-decorrelation angiography algorithm identifies vessels with flow greater than a minimum velocity. With a 70-kHz OCT system and 304 A-scans per B-scan, it should be sensitive to normal capillary flow speeds (0.4-3 mm/s).[15,16] Absence of flow signal can occur at regions of low OCT reflectance such as beneath large retinal vessels. We accounted for this by masking retinal vessels and discounting those pixels during quantification.

Conclusions

En face multimodal imaging with OCTA reveals a range of CC alterations in choroideremia and suggests that RPE loss precedes photoreceptor loss. Optical coherence tomography angiography of the CC represents a new tool for the study of chorioretinal diseases and may provide additional insights into this important vascular plexus.

Supplementary Material

Refer to Web version on PubMed Central for supplementary material.

Acknowledgments

Funding/Support: This work was supported by grants DP3 DK104397 (Dr Jia), R01EY024544 (Drs Jia and Gao), R01EY023285 (Drs Huang and Gao), 1K08 EY0231186-01 (Dr Gao), DP3 DK104397 (Dr Gao), T32 EY23211 (Dr Gao). and 1K08 EY021186-01 (Dr Pennesi), core grant P30EY010572 to Casey Eye Institute, Oregon Health & Science University, and Clinical and Translational Science Award UL1TR000128 (Drs Gao and Huang) from the National Institutes of Health; Career Development Award CF-CL-0614-0647-OHSU (Drs Jain and Gao), Enhanced Career Development Award (Dr Pennesi), and a center grant (Dr Weleber) from the Foundation Fighting Blindness; a Career Development Award (Drs Jia, Gao, and Pennesi) and an unrestricted grant to Casey Eye Institute, Oregon Health & Science University from Research to Prevent Blindness; a grant from Optovue, Inc (Dr Huang); and a grant from the Choroideremia Research Foundation (Dr Pennesi).

Role of the Funder/Sponsor: The funders had no role in the design and conduct of the study; collection, management, analysis, and interpretation of the data; preparation, review, or approval of the manuscript; and decision to submit the manuscript for publication.

References

1. Cameron JD, Fine BS, Shapiro I. Histopathologic observations in choroideremia with emphasis on vascular changes of the uveal tract. Ophthalmology. 1987; 94(2):187–196. [PubMed: 3574884]
2. Syed N, Smith JE, John SK, Seabra MC, Aguirre GD, Milam AH. Evaluation of retinal photoreceptors and pigment epithelium in a female carrier of choroideremia. Ophthalmology. 2001; 108(4):711–720. [PubMed: 11297488]
3. Jacobson SG, Cideciyan AV, Sumaroka A, et al. Remodeling of the human retina in choroideremia: rab escort protein 1 (*REP-1*) mutations. Invest Ophthalmol Vis Sci. 2006; 47(9):4113–4120. [PubMed: 16936131]
4. Tolmachova T, Anders R, Abrink M, et al. Independent degeneration of photoreceptors and retinal pigment epithelium in conditional knockout mouse models of choroideremia. J Clin Invest. 2006; 116(2):386–394. [PubMed: 16410831]
5. Tolmachova T, Wavre-Shapton ST, Barnard AR, MacLaren RE, Futter CE, Seabra MC. Retinal pigment epithelium defects accelerate photoreceptor degeneration in cell type-specific knockout mouse models of choroideremia. Invest Ophthalmol Vis Sci. 2010; 51(10):4913–4920. [PubMed: 20445111]
6. MacLaren RE, Groppe M, Barnard AR, et al. Retinal gene therapy in patients with choroideremia: initial findings from a phase 1/2 clinical trial. Lancet. 2014; 383(9923):1129–1137. [PubMed: 24439297]
7. World Medical Association. World Medical Association Declaration of Helsinki: ethical principles for medical research involving human subjects. JAMA. 2013; 310(20):2191–2194. DOI: 10.1001/jama.2013.281053 [PubMed: 24141714]
8. Jia Y, Tan O, Tokayer J, et al. Split-spectrum amplitude-decorrelation angiography with optical coherence tomography. Opt Express. 2012; 20(4):4710–4725. [PubMed: 22418228]
9. Jia Y, Bailey ST, Hwang TS, et al. Quantitative optical coherence tomography angiography of vascular abnormalities in the living human eye. Proc Natl Acad Sci USA. 2015; 112(18):E2395–E2402. [PubMed: 25897021]

10. Gao SS, Liu G, Huang D, Jia Y. Optimization of the split-spectrum amplitude-decorrelation angiography algorithm on a spectral optical coherence tomography system. Opt Lett. 2015; 40(10): 2305–2308. [PubMed: 26393725]
11. McCulloch DL, Marmor MF, Brigell MG, et al. ISCEV Standard for full-field clinical electroretinography (2015 update). Doc Ophthalmol. 2015; 130(1):1–12. [PubMed: 25502644]
12. Jia Y, Morrison JC, Tokayer J, et al. Quantitative OCT angiography of optic nerve head blood flow. Biomed Opt Express. 2012; 3(12):3127–3137. [PubMed: 23243564]
13. Liang KY, Zeger SL. Longitudinal data analysis using generalized linear models. Biometrika. 1986; 73(1):13–22. DOI: 10.1093/biomet/73.1.13
14. Schaal KB, Freund KB, Lifts KM, Zhang Y, Messinger JD, Curcio CA. Outer retinal tubulation in advanced age-related macular degeneration: optical coherence tomographic findings correspond to histology. Retina. 2015; 35(7):1339–1350. [PubMed: 25635579]
15. Tokayer J, Jia Y, Dhalla AH, Huang D. Blood flow velocity quantification using split-spectrum amplitude-decorrelation angiography with optical coherence tomography. Biomed Opt Express. 2013; 4(10):1909–1924. [PubMed: 24156053]
16. Tarn J, Tiruveedhula P, Roorda A. Characterization of single-file flow through human retinal parafoveal capillaries using an adaptive optics scanning laser ophthalmoscope. Biomed Opt Express. 2011; 2(4):781–793. [PubMed: 21483603]

Key Points

Question

What are the primary sites of tissue degeneration in choroideremia?

Findings

In this clinical case series of patients with choroideremia as well as choroideremia carriers, multimodal imaging including optical coherence tomography angiography demonstrated that retinal pigment epithelium loss exceeded photoreceptor loss in nearly all eyes. The mean choriocapillaris density was significantly lower in patients than in carriers and controls. In both patients and carriers, choriocapillaris density was significantly greater underlying regions with photoreceptor preservation as opposed to regions with photoreceptor loss.

Meaning

In vivo study of this rare disease with multimodal imaging has implications for novel treatments such as gene therapy.

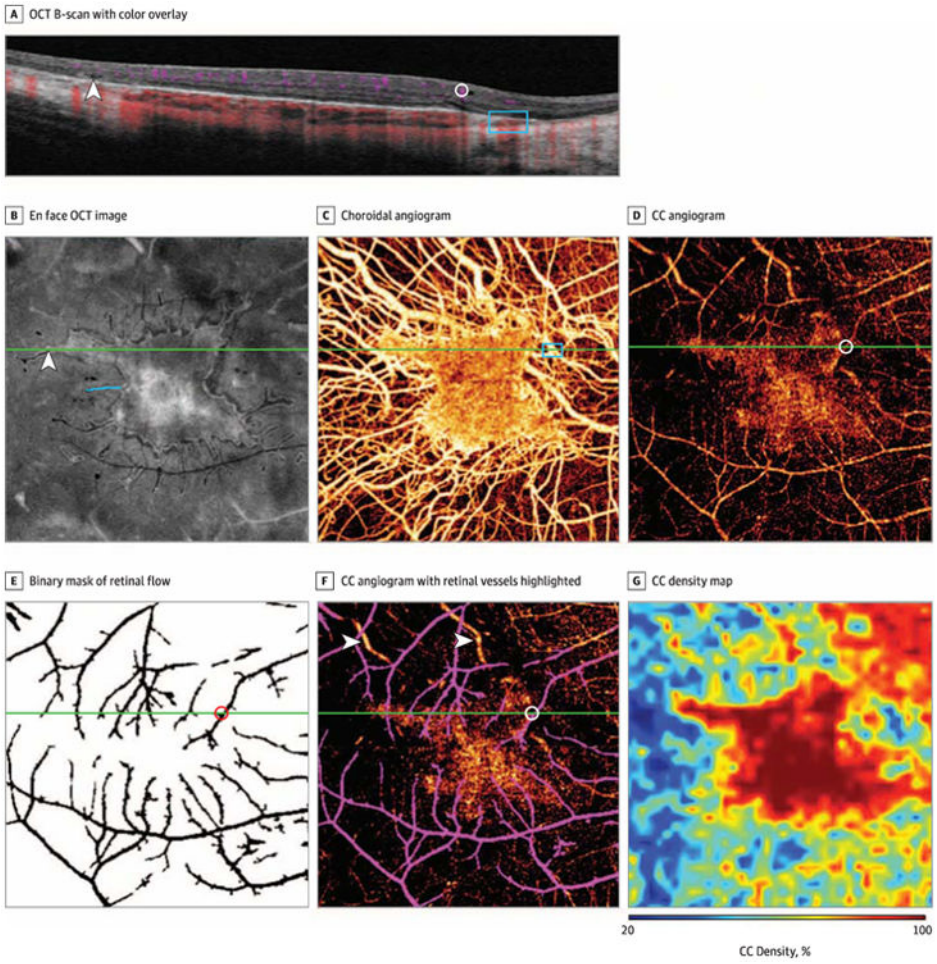

Figure 1. Multimodal Imaging in a Man in His Mid-30s With Choroideremia

A, A 6-mm optical coherence tomography (OCT) B-scan with color overlay of flow signal (purple indicates retinal flow; red, choroidal flow). There is an abrupt transition zone between intact and atrophic retinal pigment epithelium and outer retina. An outer retinal tabulation (arrowhead), captured at an oblique angle, is present lateral to the region of intact retinal pigment epithelium. A prominent inner retinal vessel (circle) projects a dynamic shadow on deeper layers. Larger choroidal vessels (rectangle) abut the Bruch membrane in areas of choriocapillaris (CC) atrophy. B, En face OCT image of the segmented outer retina capturing the ellipsoid zone reflectivity, demonstrating a central island of relatively preserved ellipsoid zone with pseudopodial extensions. An oblique B-scan section through a pseudopod (arrowhead) corresponds to the outer retinal tubulation in panel A. Pseudopod length was measured as indicated with the blue line. B-F, Green line indicates they-position of the B-scan in panel A. C, Choroidal angiogram demonstrating a central area of relatively intact CC with exposure of larger choroidal vessels in areas of CC atrophy (rectangle indicates choroidal vessels indicated by corresponding rectangle in panel A). D, Choriocapillaris angiogram obtained by segmentation of the decorrelation signal at the level of the CC, demonstrating that the greatest vessel density is associated with regions of intact outer retina. This image contains projection artifact from flow in large retinal vessels. D-F, Circle indicates the large retinal vessel from corresponding cirde in panel A. E, Binary mask

of retinal flow. Black pixels within this mask, consisting of 9.1 % of the total number of pixels, are excluded in CC density calculations. F, Same image as in panel D with retinal vessels shown in purple for clarity. Large choroidal vessels (arrowheads) remain apparent in this CC angiogram owing to extensive CC atrophy. G, Mapping of CC density, showing regions of low CC density. Pixels containing retinal flow projection artifact are treated as empty pixels for density map generation.

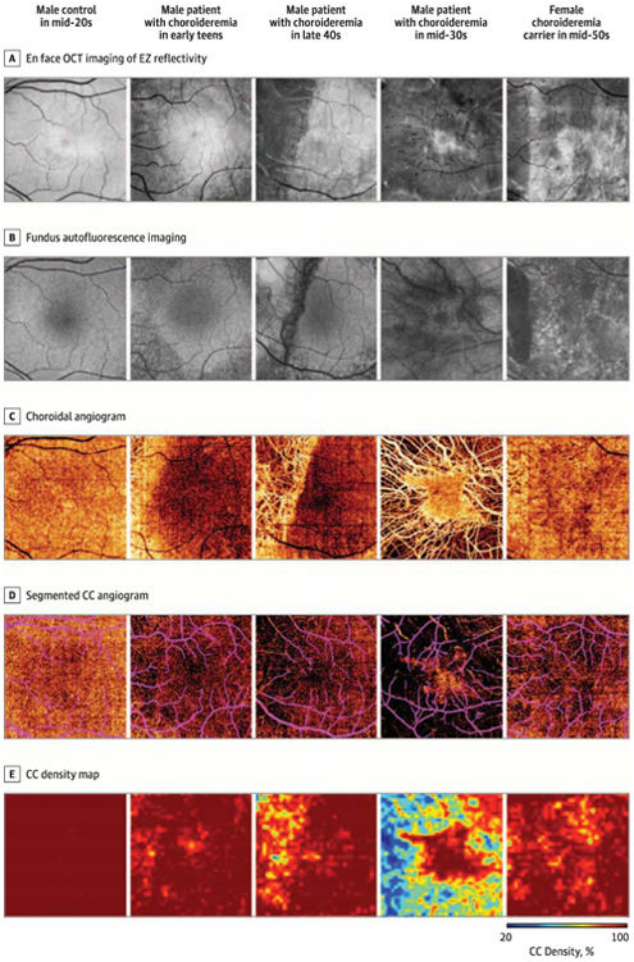

Figure 2. Range of Choriocapillaris (CC and Retinal Pigment Epithelium Alterations in Patients and Carriers in Coregistered Images

A, En face optical coherence tomography (OCT) of ellipsoid zone (EZ) reflectivity demonstrates progressive EZ loss. B, Fundus autofluorescence imaging demonstrates relative preservation of retinal pigment epithelium autofluorescence corresponding to regions of intact EZ. Retinal pigment epithelium loss is more extensive than EZ loss in nearly all eyes. C, Choroidal angiogram demonstrates increasing degrees of CC atrophy with exposure of underlying choroidal vessels. D, Segmented CC angiogram demonstrates that CC density is subnormal in affected eyes throughout tine imaged field but is worse underlying regions of EZ and retinal pigment epithelium loss. Projection artifact from large inner retinal vessels is indicated in purple. E, Mapping of CC density highlights areas of CC loss.

Table

Clinical and Imaging Findings

					Estimated Choriocapillaris Density by Region, %[a]			Area of Preserved Tissue, mm^2[a]		Pseudopod Characteristics by En Face OCT Imaging	
Participant No.	Sex	Molecular Findings	Eye	BCVA	Total	Under Regions With Intact EZ	Under Regions With Absent EZ	Outer Retinal EZ	RPE[b]	Pseudopods, No.	Longest Pseudopod, mm
CHM02	Male	Nonsense mutation (C.787C>T)	OD	20/25	58.7	86.1	52.8	6.3	3.7	20	1.24
			OS	20/25	61.7	81.9	57.7	6.0	3.8	18	1.68
CHM03	Female	Frameshift mutation (c.898dupA)	OD	20/20	94.4	94.7	93.4	28.6	28.4	3	1.44
			OS	20/20	95.9	96.2	92.2	30.3	27.9	2	0.61
CHM04	Male	Nonsense mutation (C.969T>A)	OD	20/25	74.4	91.2	70.1	NA	NA	19	1.07
			OS	20/20	66.2	86.7	61.7	NA	NA	26	1.22
CHM05	Female	Missense mutation (c.484G>A)	OD	20/50	94.2	94.7	67.7	31.5	31.4	0	0.00
			OS	20/60	87.4	95.7	71.8	22.1	19.9	12	0.73
CHM06	Male	Chromosomal duplication involving *CHM*	OD	20/15	93.8	97.8	82.2	23.0	19.6	12	0.64
			OS	20/20	94.5	98.5	85.9	24.6	23.0	8	1.18
CHM07	Male	Frameshift mutation (c.914dupG)	OD	20/25	84.1	93.3	76.6	16.0	14.4	13	1.76
			OS	20/20	83.6	93.2	76.2	15.7	10.5	24	1.39
CHM08	Male	Nonsense mutation (c.971T>G)	OD	20/20	98.7	98.7	94.1	35.8	36.0	0	0.00
			OS	20/20	98.5	98.6	92.6	35.3	36.0	1	0.20
CHM09	Male	Frameshift mutation (c.898dupA)	OD	20/20	95.6	98.7	89.9	22.7	19.9	12	0.25
			OS	20/20	89.3	93.9	77.6	26.0	24.4	14	0.30
CHM10	Male	Frameshift mutation (4-bp deletion at exon 8)	OD	20/20	82.4	93.5	72.0	17.2	12.9	7	0.88
			OS	20/50	79.2	84.2	73.3	NA	NA	10	0.49

Abbreviations: BCVA. best-corrected visual acuity; bp, base pair; EZ, ellipsoid zone; NA, not available; OCT, optical coherence tomography; RPE, retinal pigment epithelium.

[a]Measurements obtained within a 6 × 6-mm area centered on the fovea.

[b]On fundus autofluorescence.